

NANOSCIENCE AND NANOTECHNOLOGY SERIES

Transmission Electron Microscopy in Micro-nanoelectronics

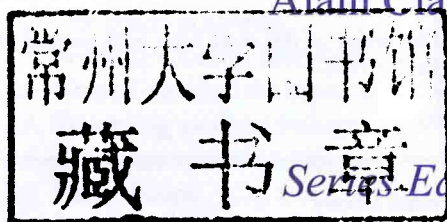
Edited by Alain Claverie

ISTE

 **WILEY**

Transmission Electron Microscopy in Micro-nanoelectronics

Edited by
Alain Claverie



Series Editor
Mireille Mouis

ISTE

 WILEY

First published 2013 in Great Britain and the United States by ISTE Ltd and John Wiley & Sons, Inc.

Apart from any fair dealing for the purposes of research or private study, or criticism or review, as permitted under the Copyright, Designs and Patents Act 1988, this publication may only be reproduced, stored or transmitted, in any form or by any means, with the prior permission in writing of the publishers, or in the case of reprographic reproduction in accordance with the terms and licenses issued by the CLA. Enquiries concerning reproduction outside these terms should be sent to the publishers at the undermentioned address:

ISTE Ltd
27-37 St George's Road
London SW19 4EU
UK

www.iste.co.uk

John Wiley & Sons, Inc.
111 River Street
Hoboken, NJ 07030
USA

www.wiley.com

© ISTE Ltd 2013

The rights of Alain Claverie to be identified as the author of this work have been asserted by him in accordance with the Copyright, Designs and Patents Act 1988.

Library of Congress Control Number: 2012952185

British Library Cataloguing-in-Publication Data

A CIP record for this book is available from the British Library

ISBN: 978-1-84821-367-8



Printed and bound in Great Britain by CPI Group (UK) Ltd, Croydon, Surrey CR0 4YY

Introduction

The MOS (Metal Oxide Semiconductor) transistor is the key component driving the electronic logic revolution for the past 50 years ever since what has become known as Moore's law was first published [MOR 65]. Moore claimed that the number of components inside a single chip would rise exponentially, increasing by a factor of two every year and a half. After 50 years and 30 technology nodes, and despite the fact that some physicists had predicted a real MOS limit for 50 nm gate lengths and below, Moore's law still does not show any inflexion. The transistor gate length has continued to decrease from a few microns to a few tens of nanometers and the number of components per chip has crossed over the billions. This trend continues at a constant speed, respecting the initial Moore's law. Why then are the limitations predicted in the literature still not observed? First, these limitations were based on the idea that evolution was only a matter of scaling and that ultimate transistors would look like the old transistors, that is planar, mostly made up of conventional Si and SiO₂ and fabricated using basically the same processes of that in the 1980s. In fact, transistors still evolve because new materials are being integrated; they are built following new architectural rules and fabricated using different, alternative, processes.

Although the "scaling down" evolution was accompanied, and sometimes even guided, by process simulations that were based on robust, well-understood and physics-based modeling, today's evolution is more complex, sometimes looking erratic, and involves exotic materials of uncertain physical and chemical characteristics, packed together using processes in which thermodynamics plays at best a second role. More than ever before, it is necessary to experimentally access the exact chemical composition and the crystalline state of these components with an extraordinary sensitivity and at nanometer resolution. This is the prerequisite condition, which is used not only to validate technological options, but most importantly to invent and calibrate the new generation of process simulators that will again be needed to continue the incredible adventure of microelectronics.

At the same time, transmission electron microscopy (TEM) is experiencing a revolution. For many years, TEM, seen by some as the last avatar of the optical

microscope, had pursued the dream of “seeing the atoms”, concentrating mostly on improving the spatial resolution. Well, this is done, and no one doubts that high-resolution TEM did help considerably in figuring out how materials are made. However, today’s availability of highly coherent electron sources, sensitive detectors, imaging filters and particularly aberration correctors has radically changed the type and quality of the information that can be obtained by TEM.

The first revolution comes from the “possibility to image fields” using electron holography. The possibility of quantifying, and mapping, electrostatic fields within a device is a smart answer to the everlasting question of “where are the active dopant atoms?” Mapping the strain fields introduced in the channel of a device to boost carrier mobility is mandatory to understand and optimize its performance. Moreover, the combination of intense nanoprobe and sensitive detectors can be used to dose impurity contents and identify chemical compounds that may form, intentionally or not, in the course of processing.

This book aims to present in a simple and practical way the new quantitative techniques based on TEM that have been recently invented or developed to address most of the challenging issues scientists and process engineers face to characterize or optimize semiconductor layers and devices. Several of these techniques are based on electron holography; others take advantage of the possibility to focus on intense beams within nanoprobe. Strain measurements and mappings, dopant activation and segregation, interfacial reactions at the nanoscale, defects identification, in situ experiments and specimen preparation by Focused Ion Beam (FIB) are among the topics presented in this book. After a brief presentation of the underlying theory, each technique is illustrated through examples from the lab or from the fab.

TEMs are now present in large numbers not only in academic but also in industrial research centers and fabrication plants. Some of the techniques introduced above and extensively described in the following chapters are not widespread, sometimes suffering from the *a priori* statement that they are “difficult”. We believe that it is not the case and hope to convince every reader, scientist or engineer to set up and use these techniques in his or her own environment taking advantage of the “existing” or “to be bought soon” equipment.

The authors of this book have lots of experience in characterizing “real” devices, answering materials science questions arising when trying to accompany, sometimes guide, technological developments aimed at rendering electronic devices smaller, faster and cheaper while consuming less energy. This experience has been gained through daily work in public (CNRS and CEA) or private (STMicroelectronics) laboratories, often collaborating together within projects or networks financially supported by several institutions among which we want to cite the European Commission (FP6 then FP7 programs), the French ANR (White and R2N programs)

and MINEFI (Alliance Nano2012) and the CNRS (METSA Network). We sincerely thank all of them for their support and help in developing and installing TEM as the indispensable companion tool of research and industry along the nanoelectronics pathway.

Bibliography

[MOR 65] MOORE G. E., "Cramming more components onto integrated circuits", *Electronics*, vol. 38, no. 8, pp. 114–117, April 1965.

Table of Contents

Introduction	xi
Chapter 1. Active Dopant Profiling in the TEM by Off-Axis Electron Holography	1
David COOPER	
1.1. Introduction	1
1.2. The Basics: from electron waves to phase images	3
1.2.1. Electron holography for the measurement of electromagnetic fields	3
1.2.2. The electron source	6
1.2.3. Forming electron holograms using an electron biprism	6
1.2.4. Care of the electron biprism	10
1.2.5. Recording electron holograms	11
1.2.6. Hologram reconstruction	12
1.2.7. Phase Jumps	15
1.3. Experimental electron holography	16
1.3.1. Fringe contrast, sampling and phase sensitivity	16
1.3.2. Optimizing the beam settings for an electron holography experiment	20
1.3.3. Optimizing the field of view using free lens control	21
1.3.4. Energy filtering for electron holography	24
1.3.5. Minimizing diffraction contrast	25
1.3.6. Measurement of the specimen thickness	26
1.3.7. Specimen preparation	28
1.3.8. The electrically inactive thickness	30
1.4. Conclusion	33
1.5. Bibliography	33

Chapter 2. Dopant Distribution Quantitative Analysis Using STEM-EELS/EDX Spectroscopy Techniques	37
Roland PANTEL and Germain SERVANTON	
2.1. Introduction.	37
2.1.1. Dopant analysis challenges in the silicon industry	37
2.1.2. The different dopant quantification and imaging methods.	38
2.2. STEM-EELS-EDX experimental challenges for quantitative dopant distribution analysis	41
2.2.1. Instrumentation present state-of-the-art and future challenges	41
2.3. Experimental conditions for STEM spectroscopy impurity detection.	43
2.3.1. Radiation damages	43
2.3.2. Particularities of EELS and EDX spectroscopy techniques	44
2.3.3. Equipments used for the STEM-EELS-EDX analyses presented in this chapter.	49
2.4. STEM EELS-EDX quantification of dopant distribution application examples	49
2.4.1. EELS application analysis examples	49
2.4.2. EDX application analysis examples	54
2.5. Discussion on the characteristics of STEM-EELS/EDX and data processing	59
2.6. Bibliography	59
Chapter 3. Quantitative Strain Measurement in Advanced Devices: A Comparison Between Convergent Beam Electron Diffraction and Nanobeam Diffraction	65
Laurent CLÉMENT and Dominique DELILLE	
3.1. Introduction.	65
3.2 Electron diffraction technique in TEM (CBED and NBD)	66
3.2.1. CBED patterns acquisition and analysis	66
3.2.2. NBD patterns acquisition and analysis	70
3.3. Experimental details.	71
3.3.1. Instrumentation and setup	71
3.3.2. Samples description	72
3.4. Results and discussion	72
3.4.1. Strain evaluation in a pMOS transistor integrating eSiGe source and drain – a comparison of CBED and NBD techniques	72
3.4.2. Quantitative strain measurement in advanced devices by NBD	75
3.5. Conclusion	78
3.6. Bibliography	78

Chapter 4. Dark-Field Electron Holography for Strain Mapping	81
Martin HÏTCH, Florent HOUELLIER, Nikolay CHERKASHIN, Shay REBOH, Elsa JAVON, Patrick BENZO, Christophe GATEL, Etienne SNOECK and Alain CLAVERIE	
4.1. Introduction.	81
4.2. Setup for dark-field electron holography	83
4.3. Experimental requirements.	85
4.4. Strained silicon transistors with recessed sources and drains stressors	87
4.4.1. Strained silicon p-MOSFET	87
4.5. Thin film effect	92
4.6. Silicon implanted with hydrogen	93
4.7. Strained silicon n-MOSFET	94
4.8. Understanding strain engineering	96
4.9. Strained silicon devices relying on stressor layers	97
4.10. 28-nm technology node MOSFETs	99
4.11. FinFET device	101
4.12. Conclusions	103
4.13. Bibliography	103
Chapter 5. Magnetic Mapping Using Electron Holography	107
Etienne SNOECK and Christophe GATEL	
5.1. Introduction.	107
5.2. Experimental	108
5.2.1. The Lorentz mode	110
5.2.2 The " ϕ^E " problem.	111
5.3. Hologram analysis: from the phase images to the magnetic properties.	118
5.3.1. The simplest case: homogeneous specimen of constant thickness.	119
5.3.2. The general case	122
5.4. Resolutions	124
5.4.1. Magnetic measurements accuracy	124
5.4.2. Spatial resolution	126
5.5. One example: FePd (L10) epitaxial thin film exhibiting a perpendicular magnetic anisotropy (PMA)	126
5.6. Prospective and new developments.	130
5.6.1. Enhanced signal and resolution.	130
5.6.2. In-situ switching	131
5.7. Conclusions.	132
5.8. Bibliography	133

Chapter 2. Dopant Distribution Quantitative Analysis**Using STEM-EELS/EDX Spectroscopy Techniques 37**

Roland PANTEL and Germain SERVANTON

2.1. Introduction.	37
2.1.1. Dopant analysis challenges in the silicon industry	37
2.1.2. The different dopant quantification and imaging methods.	38
2.2. STEM-EELS-EDX experimental challenges for quantitative dopant distribution analysis	41
2.2.1. Instrumentation present state-of-the-art and future challenges	41
2.3. Experimental conditions for STEM spectroscopy impurity detection.	43
2.3.1. Radiation damages	43
2.3.2. Particularities of EELS and EDX spectroscopy techniques	44
2.3.3. Equipments used for the STEM-EELS-EDX analyses presented in this chapter.	49
2.4. STEM EELS-EDX quantification of dopant distribution application examples	49
2.4.1. EELS application analysis examples	49
2.4.2. EDX application analysis examples	54
2.5. Discussion on the characteristics of STEM-EELS/EDX and data processing	59
2.6. Bibliography	59

**Chapter 3. Quantitative Strain Measurement in Advanced Devices: A
Comparison Between Convergent Beam Electron Diffraction and
Nano-beam Diffraction 65**

Laurent CLÉMENT and Dominique DELILLE

3.1. Introduction.	65
3.2 Electron diffraction technique in TEM (CBED and NBD)	66
3.2.1. CBED patterns acquisition and analysis	66
3.2.2. NBD patterns acquisition and analysis	70
3.3. Experimental details.	71
3.3.1. Instrumentation and setup	71
3.3.2. Samples description	72
3.4. Results and discussion	72
3.4.1. Strain evaluation in a pMOS transistor integrating eSiGe source and drain – a comparison of CBED and NBD techniques	72
3.4.2. Quantitative strain measurement in advanced devices by NBD	75
3.5. Conclusion	78
3.6. Bibliography	78

Chapter 4. Dark-Field Electron Holography for Strain Mapping	81
Martin HÛTCH, Florent HOUELLIER, Nikolay CHERKASHIN, Shay REBOH, Elsa JAVON, Patrick BENZO, Christophe GATEL, Etienne SNOECK and Alain CLAVERIE	
4.1. Introduction.	81
4.2. Setup for dark-field electron holography	83
4.3. Experimental requirements.	85
4.4. Strained silicon transistors with recessed sources and drains stressors	87
4.4.1. Strained silicon p-MOSFET	87
4.5. Thin film effect	92
4.6. Silicon implanted with hydrogen	93
4.7. Strained silicon n-MOSFET	94
4.8. Understanding strain engineering	96
4.9. Strained silicon devices relying on stressor layers	97
4.10. 28-nm technology node MOSFETs	99
4.11. FinFET device	101
4.12. Conclusions	103
4.13. Bibliography	103
Chapter 5. Magnetic Mapping Using Electron Holography	107
Etienne SNOECK and Christophe GATEL	
5.1. Introduction.	107
5.2. Experimental	108
5.2.1. The Lorentz mode	110
5.2.2 The " ϕ^E " problem.	111
5.3. Hologram analysis: from the phase images to the magnetic properties.	118
5.3.1. The simplest case: homogeneous specimen of constant thickness.	119
5.3.2. The general case	122
5.4. Resolutions	124
5.4.1. Magnetic measurements accuracy	124
5.4.2. Spatial resolution	126
5.5. One example: FePd (L10) epitaxial thin film exhibiting a perpendicular magnetic anisotropy (PMA)	126
5.6. Prospective and new developments.	130
5.6.1. Enhanced signal and resolution.	130
5.6.2. In-situ switching	131
5.7. Conclusions.	132
5.8. Bibliography	133

Chapter 6. Interdiffusion and Chemical Reaction at Interfaces by TEM/EELS	135
Sylvie SCHAMM-CHARDON	
6.1. Introduction.	135
6.2. Importance of interfaces in MOSFETs.	135
6.3. TEM and EELS	137
6.4. TEM/EELS and study of interdiffusion/chemical reaction at interfaces in microelectronics	137
6.4.1. Thickness measurement	138
6.4.2. Atomic structure analysis	139
6.4.3. EELS analysis	141
6.4.4. Sample preparation	143
6.5. HRTEM/EELS as a support to developments of RE- and TM-based HK thin films on Si and Ge	144
6.5.1. Introduction	144
6.5.2. HRTEM/EELS methodology	145
6.5.3. Illustrations	154
6.6. Conclusion	158
6.7 Bibliography	158
Chapter 7. Characterization of Process-Induced Defects.	165
Nikolay CHERKASHIN and Alain CLAVERIE.	
7.1. Interfacial dislocations	166
7.1.1. Si(100)/Si(100) direct wafer bonding (DWB)	167
7.1.2. SiGe heterostructures	170
7.2. Ion implantation induced defects	172
7.2.1. Defects of interstitial type	173
7.2.2. Defects of vacancy type	187
7.3. Conclusions.	193
7.4. Bibliography	193
Chapter 8. <i>In Situ</i> Characterization Methods in Transmission Electron Microscopy	199
Aurélien MASSEBOEUF	
8.1. Introduction.	199
8.2. <i>In situ</i> in a TEM	200
8.2.1. Temperature control and irradiation	201
8.2.2. Electromagnetic field	201
8.2.3. Mechanical.	202
8.2.4. Chemistry	202
8.2.5. Light	203
8.2.6. Multiple and movable currents	203

8.3. Biasing in a conventional TEM	204
8.3.1. Multiple contacts	204
8.3.2. Movable contacts	206
8.3.3. Comparison	206
8.4. Sample design	208
8.4.1. Focused ion beam.	208
8.4.2. TEM windows.	209
8.5. Conclusions.	211
8.6. Bibliography	211
Chapter 9. Specimen Preparation for Semiconductor Analysis.	219
David COOPER and Gérard BEN ASSAYAG	
9.1. The focused ion beam tool	220
9.2. Ion-sample interaction	221
9.3. Beam currents and energies for specimen preparation.	225
9.4. Practical specimen preparation	228
9.5. In situ lift-out.	228
9.6. H-bar technique	232
9.7. Broad beam ion milling.	233
9.8. Mechanical wedge polishing.	235
9.9. Conclusion	235
9.10 Bibliography.	236
List of Authors	237
Index	241

Chapter 1

Active Dopant Profiling in the TEM by Off-Axis Electron Holography

1.1. Introduction

Electron holography is a powerful transmission electron microscopy (TEM)-based technique that can be used to measure the phase change of an electron wave that has passed through a region of interest compared to the phase of an electron wave that has passed through only a vacuum. As the phase of an electron is sensitive to the magnetic, electrostatic and strain fields that can be found in and around a specimen, electron holography is a unique method that can be used to recover all of these properties with nanometer-scale resolution. The electrostatic potential in semiconductor materials is modified by the presence of active dopants. At this time, when only a few dopant atoms can affect the properties of an electronic device, electron holography provides a unique opportunity to look inside these devices and to learn about the activity of the dopant atoms. Characterization techniques such as secondary ion mass spectrometry and atom probe tomography cannot differentiate between active and inactive dopants. Other techniques such as scanning capacitance microscopy and scanning spreading resistance microscopy, which are capable of measuring the active dopants at the surface of specimens, may well have problems adapting to the latest generations of semiconductor materials that can consist of doped nanowires and three-dimensional structures. Therefore, electron holography is unique in that it allows the position of active dopants to be measured inside a specimen with 1 nm spatial resolution today [COO 11], and potentially atomic resolution in the future.

It was Gabor who introduced electron holography in his paper “Microscopy by Reconstructed Wavefronts” in 1948 [GAB 48]. Gabor realized that the measurement of the phase of an electron beam would allow the aberrations of an optical system to be eliminated. These ideas have been used in what is now known as high-resolution electron holography that have provided the first examples of sub-Ångström imaging [ORC 95]. Today, electron holography is used to describe any method that allows both the amplitude and phase information that is contained in an electron wave to be reconstructed. There are many different methods for performing electron holography, notably in-line holography that has been successfully used for the characterization of strain, dopant and magnetic fields. However, it is off-axis electron holography that is the most widely used. For simplicity, from now on, it will be referred to as electron holography. Here, a Mollenstedt–Duker biprism is used; this is a charged wire, normally located in the selected area aperture plane in a microscope. The biprism is used to tilt a reference wave so that it interferes with an object wave to provide an interference pattern in the image plane. From this interference pattern, which is also known as the electron hologram, the phase of the electron wave can be reconstructed. It was not until the 1980s when groups led by Tonomura, Pozzi and Lichte began to successfully use electron holography to solve materials science problems. However, the invention of stable and coherent electron sources in the 1990s finally allowed electron holography to become more widespread. Indeed, using the latest, ultrastable electron microscopes in 2012, electron holography has become a much more user-friendly technique that provides the microscopist with wonderful opportunities to solve materials science problems that are not available elsewhere.

This chapter is designed to show the reader how to perform electron holography in a transmission electron microscope and then how to use electron holography for dopant profiling. There are many books and reviews that deal with the theory and background in detail that should be consulted for a more complete discussion of the aspects discussed here. This chapter is designed to provide a “hands-on” approach regarding electron holography that will allow the readers to be able to get the most out of their microscope and avoid many of the common and not-so-well-known problems that can be encountered when performing electron holography.

Experimental results have been used to illustrate everything that is discussed here. The experimental conditions have been kept as constant as possible. All examples shown here were acquired using an FEI Titan TEM operated at 200 kV. Unless otherwise discussed, the Lorentz lens was used with the conventional objective lens switched off. Although the microscope used here has a probe corrector, it was not used. The presence of the probe corrector meant that the third conventional lens was switched off in order to be able to achieve the astigmatism that is required for electron holography. For recording the electron holograms, a charge-coupled device (CCD) camera attached to a Gatan energy filter was used.

This provides convenience as the image is observed at a low magnification on the TEM viewing screen to allow the whole of the sample, beam and biprism to be observed at the same time with the additional magnification then provided in the energy filter. In addition, the energy filter can be used to improve the hologram contrast. Unless otherwise stated, a $2,048 \times 2,048$ pixel CCD camera was used in "double binning" mode to provide $1,024 \times 1,024$ pixel images. Although the examples shown were acquired using a Titan TEM, everything discussed in this chapter can be transferred to any other type of TEM that is equipped with an electron biprism in the selected area plane.

1.2. The Basics: from electron waves to phase images

1.2.1. Electron holography for the measurement of electromagnetic fields

The phase of an electron wave that has passed through a specimen will be changed by the electromagnetic field. This phase change is given by:

$$\phi(x) = C_E \iint V(x, z) dz - \frac{e}{\hbar} \iint B_{\perp}(x, z) dx dz$$

where z is the direction of the incident electron beam, x is the direction in the plane of the specimen, V_0 is the electrostatic potential and B_{\perp} is the component of the magnetic induction that is perpendicular to both x and z [TON 87]. When examining specimens containing dopants, it is assumed that there is no magnetic field present. For the measurement of electrostatic potentials, the interaction constant, C_E is given by:

$$C_E = \frac{2\pi}{\lambda} \frac{E_k + E_0}{E_k(E_k + 2E_0)}$$

where λ is the electron wavelength, E_0 is the rest energy of the electron and E_k is the kinetic energy of the electron. The interaction constant is 7.29×10^6 rads $V^{-1}m^{-1}$ for 200 kV electrons and 6.53×10^6 rads $V^{-1}m^{-1}$ for 300 kV electrons. Figure 1.1 shows C_E plotted for a range of microscope operating voltages revealing that the incident electrons interact more with the electrostatic potential at lower energies.

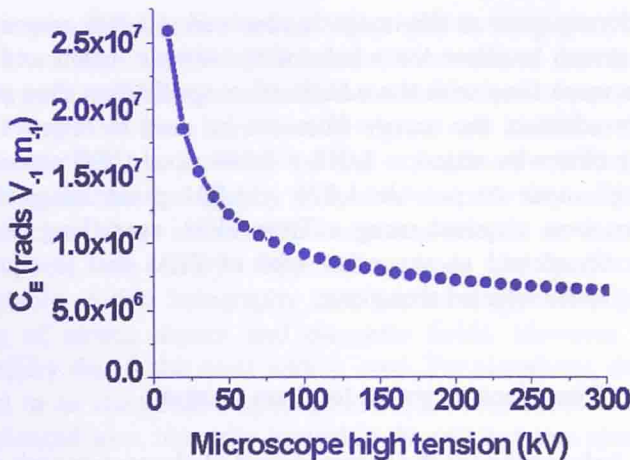


Figure 1.1. C_E as a function of the energy of the electron beam.

Following the notation of Hytch, when understanding the origin of the different phases that are measured by electron holography, we can write the phase as having four different components [HYT 11].

$$\phi_g(r) = \phi_g^G(r) + \phi_g^C(r) + \phi_g^M(r) + \phi_g^E(r)$$

where ϕ_g^G refers to the geometric phase that describes the distortion from the crystal lattice, ϕ_g^C refers to the crystalline phase resulting from the scattering of electrons from the crystal potential, ϕ_g^M is the magnetic contribution and ϕ_g^E is the contribution from the electrical fields in and around the specimen. For the purpose of this chapter, which concentrates on dopant profiling by electron holography, we will assume that the specimen is both non-magnetic and has been tilted to a weakly diffracting orientation and will only be concerned with the term $\phi_g^E(r)$. Within this term, the measured phase will have two components, the mean inner potential (MIP) V_0 and the dopant-related potential V_E .

$$V^E(r) = V_0(r) + V_E(r)$$

The MIP is defined as the volume average of the electrostatic potential in a specimen. The MIP can be calculated by using a non-binding approximation, which considers the sample as an array of neutral atoms and gives an upper limit, as it does not account for the distribution of valence electrons due to bonding. The electron